Acta Pharmaceutica Sinica B 2020;10(8):1521−1533

Chinese Pharmaceutical Association
Institute of Materia Medica, Chinese Academy of Medical Sciences

Acta Pharmaceutica Sinica B

www.elsevier.com/locate/apsb
www.sciencedirect.com

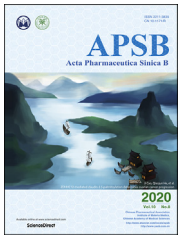

ORIGINAL ARTICLE

Intracellular codelivery of anti-inflammatory drug and anti-miR 155 to treat inflammatory disease

Chao Teng[a], Chenshi Lin[a], Feifei Huang[a], Xuyang Xing[a], Shenyu Chen[a], Ling Ye[b], Helena S. Azevedo[c], Chenjie Xu[d], Zhengfeng Wu[e], Zhongjian Chen[f], Wei He[a,f,*]

[a]*School of Pharmacy, China Pharmaceutical University, Nanjing 210009, China*
[b]*School of Pharmaceutical Sciences, Southern Medical University, Guangzhou 510515, China*
[c]*School of Engineering and Materials Science, Institute of Bioengineering, University of London, London E1 4NS, UK*
[d]*Department of Biomedical Engineering, City University of Hong Kong, Kowloon, Hong Kong, China*
[e]*Key Laboratory of Modern Preparation of TCM, Ministry of Education, Jiangxi University of Traditional Chinese Medicine, Nanchang 330004, China*
[f]*Shanghai Skin Disease Hospital, Tongji University School of Medicine, Shanghai 200443, China*

Received 12 March 2020; received in revised form 18 April 2020; accepted 25 May 2020

KEYWORDS

Codelivery;
Intracellular fate;
Nucleic acid;
Baicalein;
Macrophages;
Inflammatory disease

Abstract Atherosclerosis (AS) is a lipid-driven chronic inflammatory disease occurring at the arterial subendothelial space. Macrophages play a critical role in the initiation and development of AS. Herein, targeted codelivery of anti-miR 155 and anti-inflammatory baicalein is exploited to polarize macrophages toward M2 phenotype, inhibit inflammation and treat AS. The codelivery system consists of a carrier-free strategy (drug-delivering-drug, DDD), fabricated by loading anti-miR155 on baicalein nanocrystals, named as baicalein nanorods (BNRs), followed by sialic acid coating to target macrophages. The codelivery system, with a diameter of 150 nm, enables efficient intracellular delivery of anti-miR155 and polarizes M1 to M2, while markedly lowers the level of inflammatory factors *in vitro* and *in vivo*. In particular, intracellular fate assay reveals that the codelivery system allows for sustained drug release over time after internalization. Moreover, due to prolonged blood circulation and improved accumulation at the AS plaque, the codelivery system significantly alleviates AS in animal model by increasing the artery

*Corresponding author.
E-mail address: weihe@cpu.edu.cn (Wei He).

Peer review under the responsibility of Institute of Materia Medica, Chinese Academy of Medical Sciences and Chinese Pharmaceutical Association.

https://doi.org/10.1016/j.apsb.2020.06.005

lumen diameter, reducing blood pressure, promoting M2 polarization, inhibiting secretion of inflammatory factors and decreasing blood lipids. Taken together, the codelivery could potentially be used to treat vascular inflammation.

1. Introduction

Atherosclerosis (AS), a leading cause of death worldwide, is a lipid-driven inflammatory disease[1,2]. AS is characterized by plaque buildup at the arterial subendothelial space (intima) due to the accumulation of diseased cells including monocytes, macrophages, endothelial cells, smooth muscle cells, neutrophils, lipids, and extracellular matrix components[3–5]. The macrophages at the plaque and macrophage-derived pro-inflammatory cytokines are predominant driven-factors for the development of AS[6]. As such, targeting to macrophages may offer therapeutic opportunities to regress AS. Several approaches on macrophage targeting have been reported, such as improving cholesterol efflux, inhibition of foam cell formation, improving resolution of inflammation, and polarizing macrophages toward anti-inflammatory phenotypes (M2)[7]. Herein, we hypothesized that a strategy for promoting polarization, plus suppression of inflammation, has potential to treat AS with improved efficacy.

Macrophages, such as M1 and M2 macrophages, have a highly versatile phenotype and adapt their phenotypic alteration in response to their microenvironment of diseased site[8]. M1 macrophages are pro-inflammatory, inducing inflammation activities by secreting pro-inflammatory cytokines, reactive oxygen species (ROS), whereas M2 is an anti-inflammatory phenotype characterized by high expression of scavenging molecules, mannose and galactose receptors, ornithine, and polyamines[7]. Furthermore, M2 macrophages promote tissue remodeling and healing, increase the response to fungal infection *via* reduction of autophagy, and facilitate modulation of other immune cells in a adaptable pattern[9]. Thus, promoting switch from M1 to M2 offers the possibility to alleviate the inflammation response and treat AS. Increasing evidence suggests that overexpression of microRNA-155 (miR 155) could re-program M2 to M1 macrophages through multiple pathways, such as CCAAT-enhancer binding protein (C/EBP-β) signaling cascade[10], c-Jun N-terminal kinase (JNK) pathway[11], tumor necrosis factor α (TNF-α) and nuclear factor-kappa B (NF-κB) signaling[11], and B-cell lymphoma 6 (BCL-6) protein[12]. Inhibition of miR-155 in M1 using antisense oligonucleotides, *e.g.*, anti-miR155, was shown to facilitate M2 switch from M1[10]. Nonetheless, phenotypic polarization is a dynamic process, indicating that macrophages frequently exist in a continuum among multiple reversible phenotypes that reflects the activity of different transcriptional networks and crosstalk between these networks. Thus, a strategy of M2 polarization plus inhibition of inflammation may further benefit AS treatment[13]. Baicalein, a major flavonoid of *Scutellaria baicalensis,* is an effective anti-inflammatory drug mainly acting *via* inhibition of NF-κB[14,15]. Consequently, codelivery of anti-miR155 and baicalein is a potential method for combined therapy and treatment of AS, assuming that intracellular delivery of anti-miR155 enables M2 polarization *via* downregulation of BCL-6 and baicalein predominantly inhibits inflammation rapidly by suppressing secretion of NF-κB after dosing (Scheme 1).

However, baicalein is a poorly water-soluble drug, with a molecular weight of 270 g/mol and water-solubility of less than 0.076 mg/mL[16]. On the other hand, anti-miR 155 is a macromolecular drug characterized by high molecular weight, instability and poor membrane penetration[17], making their codelivery challenging. Furthermore, degradation by the endo-lysosomes is a critical obstacle for intracellular delivery of nucleic acid. Conventional drug delivery systems (DDS), such as liposomes and polymeric nanoparticles allow for improved intracellular delivery of biological drugs[18,19]; however, their efficacy of cytosolic delivery is low at less than 2%[20]. In our previous reports[21–24], a carrier-free platform of codelivery, drug-delivering-drug (DDD), was developed by using rod-like nanocrystals of insoluble drug with a diameter of less than 200 nm as carriers to deliver biological drugs, such as miRNAs and active proteins, to cells *via* bypassing the endo-lysosomes. In this study, anti-inflammatory baicalein nanocrystals, here referred as baicalein nanorods (BNRs), were utilized as carriers for intracellular delivery of anti-miR155 for combined treatment of AS. Anti-miR155 were complexed with BNRs, followed by sialic acid (SA) coating for targeting SA receptors on macrophages[25,26] (Scheme 1). The proposed mechanism of action is displayed in Scheme 1.

2. Materials and methods

2.1. Cell cultures and animals

RAW 264.7 cells (Nanjing KeyGEN Biotech Co., Ltd., Nanjing, China) were maintained in Dulbecco's modified Eagle's medium (DMEM) supplemented with 10% fetal bovine serum (FBS) and 1% penicillin/streptomycin at 37 °C, 5% CO_2 and 100% humidity and were split when confluent. Prior to use, the cells were polarized into M1 phenotype by incubation with lipopolysaccharides (100 ng/mL) and interferon-γ (20 ng/mL) for 24 h.

The animals used in all experiments received care in compliance with the Principles of Laboratory Animal Care and the Guide for the Care and Use of Laboratory Animals. Animal experiments followed a protocol approved by the China Pharmaceutical University Institutional Animal Care and Use Committee.

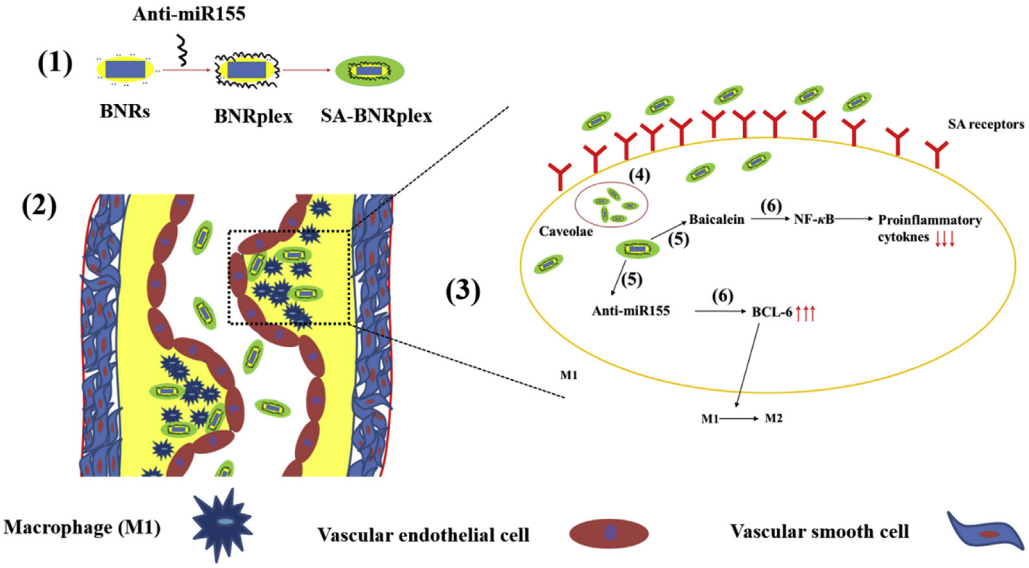

Scheme 1 Design and proposed mechanism for AS treatment through codelivery of anti-inflammatory drug baicalein and anti-miR 155 using the drug-delivering-drug (DDD) platform. (1) Preparation of BNRplex and SA-BNRplex. After i.v. administration, SA-BNRplex can (2) accumulate in the plaque, (3) target macrophages *via* binding with the SA receptors, and (4) enter the cells *via* the nonlysosomal route (caveolar endocytosis), (5) release the baicalein and anti-miR155. Finally, (6) the released baicalein inhibits the secretion of inflammatory factors by suppressing the expression of NF-κB while the dissociated anti-miR155 promotes the phenotypic switch from pro-inflammatory M1 to anti-inflammatory M2 by upregulating the BCL-6, ultimately achieving combined treatment of AS.

2.2. *Preparation and characterization of codelivery system*

The baicalein nanorods (BNRs) were prepared using CLG as a stabilizer. Cationic beta-lactoglobulin (CLG) was synthesized *via* conjugation of ethylenediamine to beta-lactoglobulin (β-LG, Sigma−Aldrich, St. Louis, MO, USA), as described in our previous reports[21−23]. Briefly, 1 mL of dimethylsulfoxide (DMSO) containing baicalein (30 mg, Chengdu Pufei De Biotech Co., Ltd., Chengdu, China) was mixed with CLG solution (10 mL, 1 mg/mL), followed by treatment in an ultrasonic probe (20−25 kHz, Scientz Biotechnology Co., Ltd., Ningbo, China) at 300 W for 15 min and evaporation under reduced pressure. BNRplex and SA-BNRplex were prepared as follows: BNRs were mixed with an equal volume solution of anti-miR 155, incubated at room temperature for 30 min, blended with SA (Sigma−Aldrich) solution at various concentrations from 0.5 to 4 mg/mL. The temperature in the entire procedure was controlled below 4 °C in an ice−water bath. Dye-labeled nanoparticles were prepared by dissolving the dye with baicalein in DMSO together as the organic phase prior to mixing with CLG protein.

Agarose gel electrophoresis was used to assess the loading of nucleic acid on the nanoparticles. In brief, the gels were prepared with 2% agarose in Tris buffer containing ethylenediaminetetraacetic acid at pH 8.0. The sampe was blended with gelRed (Generay Biotechnology, Shanghai, China) following the manufacturer's protocol, separated by gel electrophoresis at 110 V for 30 min, and ultimately imaged in a Bio-Rad high-sensitivity chemiluminescence imaging system (Chemidoc XRS+, Hercules, USA).

To assess the stability, the nanoparticles were incubated with RNase (Solarbio Science & Technology Co., Ltd., Beijing, China) or serum-containing medium at 37 °C. At predetermined time points, the samples were incubated with 1% SDS for 5 min at 60 °C, followed by addition of 2% SDS and determination by agarose gel electrophoresis.

For baicalein release *in vitro*, the nanoparticles were placed into the 3.5 kDa dialysis bag, incubated with release media with different pH values, and put in an incubator (SHA-C, Jintan, China) with a shaking speed of 100 rpm at 37 °C. Samples were withdrawn at specific time intervals, filtrated through a 0.2-μm filter and analysed by high performance liquid chromatography (HPLC, SHIMAZU LC-10AT, Kyoto, Japan) under isocratic conditions. The mobile phase was methanol/0.05% phosphoric acid (70/30, *v*/*v*) at flow rate of 1 mL/min. Stationay phase was ODS C18 column (250 mm × 4.6 mm, 5 μm, Diamonsil, Beijing, China) at 30 °C and detection was made at wavelenght of 276 nm.

2.3. *Flow cytometry and confocal microscopy imaging*

The cellular study was investigated by LSM700 confocal laser scanning microscopy (CLSM, Carl Zeiss, Jena, Germany) and flow cytometry. The cell density used was 2×10^5 cells/well. For uptake study, cells were first incubated with the nanoparticles at a Cy5 concentration of 100 nmol/L at 37 °C for 4 h (Solarbio Science & Technology Co., Ltd.). For investigation of endocytic mechanism, cells were cultured with uptake inhibitors, NaN_3 (10 mmol/L) and M-CD (2.5 mmol/L) (Aladdin Co., Ltd., Shanghai, China), for 30 min in advance. To evaluate co-localization, cells were incubated with dye-labeled nanoparticles in DMEM for 4 h at 37 °C, stained with caveolae markers, Alexa Fluor® 488-Cave-1/F-actin/CTB for 3 h, or lyso-tracker red or green for 1 h (Abcam Trading Co., Ltd., Shanghai, China), rinsed with PBS and observed by CLSM.

To determine the phenotypic shift *in vitro*, RAW 264.7 cells (1×10^5 cells/well) were incubated with different nanoparticles for 12 h, rinsed with PBS, fixed in the 4% paraformaldehyde for 10 min, permeabilized in 0.1% Triton X-100 for 10 min, blocked

in a blocking buffer for 30 min, incubated with primary antibodies at 4 °C for 2 h and a secondary antibody at 4 °C overnight, stained with DAPI for 15 min, and finally observed by CLSM.

To investigate the intracellular fate, cells (1×10^5 cells/well) were cultured with Cy5/tetraphenylethylene (TPE, Sigma−Aldrich) dual-labeled nanoparticles at 37 °C at a TPE concentration of 50 μmol/L and Cy5 of 100 nmol/L. At specific time points, the cells were observed by CLSM and assayed by flow cytometry (BD FACSCalibur, San Jose, CA, USA).

2.4. Determination of inflammatory factors

RAW 264.7 cells cultured in 6-well plate at a density of 2×10^5 cells/well were incubated with different nanoparticles for 12 h, followed by washing with PBS. The anti-inflammation effect was examined by measuring the concentration of TNF-α and IL-12 in the cell supernatant using ELISA kits (Enzyme-linked Biotechnology Co., Ltd., Shanghai, China) according to the manufacturer's instructions.

2.5. Western blot (WB)

RAW 264.7 cells cultured in 6-well plates at a density of 2×10^5 cells/well were incubated with different nanoparticles for 24 h, followed by incubation with RIPA buffers for 15 min in ice, centrifuging at 9,000×g for 10 min at 4 °C. Protein determination was performed using a BCA protein assay kit (Beyotime, Shanghai, China) and finally isolation on 10% SDS-PAGE. The separated proteins were loaded into a nitrocellulose membrane followed by incubation in blocking solution containing 5% skim milk powder at 37 °C for 2 h, rinsed with phosphate buffer solution containing Tween 20 two to three times, incubated with primary antibodies for 2 h and then secondary antibodies at 4 °C overnight, stained with a chemiluminescence kit (KeyGEN Biotech, Nanjing, China), and finally visualized with an Odyssey Infrared Imaging System (LICOR Biotechnology, Lincoln, USA). β-Actin was used as an internal control to normalize protein expression. Integrated optical density was calculated using software Image J (NIH, Bethesda, USA).

2.6. In vitro cytotoxicity

RAW 264.7 cells seeded in 96-well plates at a density of 5×10^3 cells/well were first cultured for 48 h and then incubated with drug formulations or CLG for 48 h at 37 °C. Cell viability was assessed by the standard assay of 3-(4,5-dimethylthiazol-2yl)-2,5-diphenyltetrazoliumbromide (MTT, Sigma−Aldrich).

2.7. Blood circulation and plaque targeting in vivo

AS animal model was prepared as described in previous reports[27,28]. In brief, rats were administrated with vitamin D_3 (Shanghai General Pharmaceutical Co., Ltd., Shanghai, China) *via* intraperitoneal injection for three times/3 day at 700,000 IU/kg based on the body weight, followed by feeding with high-fat diets for 4 months (2% cholesterol, 0.5% sodium cholate, 3% lard, 0.2% propylthiouracil, and 94.3% base feed).

The rats were randomly divided into four groups (5 rats per group) and were intravenously administrated with 1,1′-dioctadecyl-3,3,3′,3′-tetramethylindotricarbocyanine iodide (DiR, Biotium, Inc. Hayward, CA, USA), DiR-labeled nanoparticles (BNRs, BNRplex and SA-BNRplex) at a DiR dose of 0.5 mg/kg, according to the body weight. At specific time intervals, 0.5 mL of blood was sampled from the orbital vein and immediately centrifuged for 10 min at 5,000×g to obtain the plasma for determination of fluorescence intensity with a multi-function microplate reader (POLARstar Omega, BMG LABTECH, Ortenberg, Germany). The pharmacokinetic parameters were calculated by using the Microsoft Excel 2016 program by a statistical moment principle.

To study the accumulation of nanoparticles in the plaques, the arteries were exceised from the AS rat model at 2 h post administration of fluorescein isothiocyanate isomer I (FITC)-labeled nanoparticles, frozen, sectioned with a microtome (Leica CM1860, Wetzlar, Germany), stained with DAPI and finally observed with CLSM.

2.8. Therapeutic efficacy

The animals (AS rat model) were randomly divided into six groups ($n = 5$) and intravenously injected with various formulations (0.5 mL) every 3 days for 5 times at a baicalein dose of 5 mg/kg, atorvastatin dose of 1 mg/kg and anti-miR 155 dose of 0.2 mg/kg, according to the animal's body weight. After the treatment, blood pressure was measured with an IITC blood pressure system (IITC Life Science Inc., Woodland Hills, CA, USA), carotid arteries were collected and analyzed by Hematoxylin & Eosin Staining (H&E) staining and blood lipids were quantified by ELISA kit. The anti-inflammation effect was examined by measuring the levels of TNF-α and IL-12 in the serum using ELISA kits (Enzyme-linked Biotechnology Co., Ltd., Shanghai, China) according to the manufacturer's instructions. The level of BCL-6 was assessed *via* WB analysis.

To determine the phenotypic shift, collected samples were cut into 6−8 μm sections and then incubated with primary antibodies at 4 °C for 2 h and a secondary antibody at 4 °C overnight, stained with DAPI for 15 min, and finally observed by CLSM.

2.9. Statistical analysis

One-way analysis of variance was performed to assess the statistical significance of the differences between samples. The results are expressed as the mean ± standard deviation (SD). $P < 0.05$ indicated significant differences.

3. Results

3.1. Preparation and characterization of codelivery system

The preparation of SA-BNRplex involved three steps, including the preparation of anti-inflammatory baicalein nanocrystals (named as baicalein nanorods, BNRs) and complexation of the nanorods with -anti-miR 155 complex (BNRplex) and furter coating with sialic acid (SA) to obtain (SA-BNRplex, Scheme 1). First, BNRs were prepared by using CLG as a stabilizer by surface coating to inhibit their aggregation. Also, the coating with CLG enables BNRs to have a positive charge for complexation with negatively charged nucleic acid. To confirm the stabilization effect of CLG on BNRs, fluorescence spectroscopy was utilized based on the selective excitation of tryptophan (Trp) residues in CLG's structure at 340 nm. As displayed in Supporting Information Fig. S1, the BNRs allow for fluorescence quenching at 340 nm, independently of the drug loading, and implying the interaction

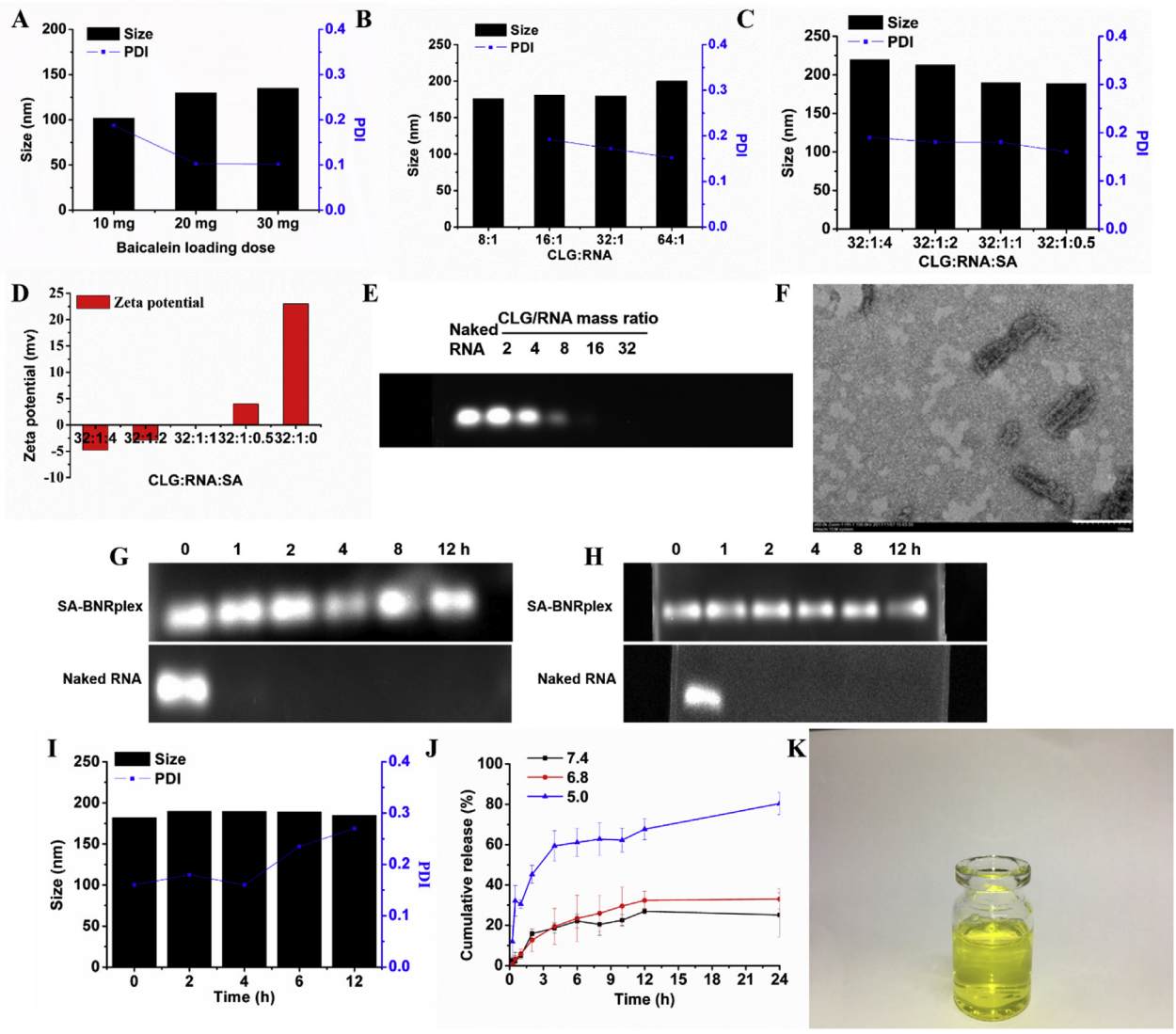

Figure 1 Characterization of SA-BNRplex. (A) Effect of baicalein-loading on the particle size of BNRs. (B) Effect of mass ratio of CLG/anti-miR 155 on the particle size of BNRplex; effect of SA coating on the (C) particle size and (D) surface zeta potential of SA-BNRplex. (E) Gel electrophoresis assay of BNRplex. (F) TEM image (scale bar = 100 nm) of optimized formulation. Stability against (G) RNase or (H) serum evaluated by agarose gel electrophoresis. Anti-miR155 or SA-BNRplex was incubated with 10% serum solution or 10 μg/mL RNase at 37 °C for different durations. (I) Particle-size change of SA-BNRplex in 10% serum solution. (J) *In vitro* release of baicalein from SA-BNRplex in buffer solution at pH of 5.0, 6.8, and 7.4 at 37 °C for 24 h (mean ± SD, $n = 3$). (K) Digital photo of optimized formulation.

between drug particles and the stabilizer. Although an increase in the amount of drug loaded, from 10 to 30 mg in 10 mL of 1 mg/mL CLG solution, contributes the increase in the particle diameter of BNRs, all sizes are smaller than 150 nm, along with PDI less than 0.2, thereby demonstrating good size uniformity (Fig. 1A). Due to high drug loading, the formulation with 75% loading of baicalein (30 mg drug in formulation, *w/w*) was selected for subsquent studies. Secondly, BNRplex was obtained by loading anti-miR155 on BNRs *via* electrostatic interaction. Native SDS page shows that, as the mass ratio of CLG/anti-miR155 is geater than 16, the bands disappear (Fig. 1E), indicating the nucleic acid was well condensed. Further increase in the mass ratio had little influence on the particle size of BNRplex (Fig. 1B). The BNRplex with mass ratio of 32 was chosen for SA coating to target SA receptors on macrophages and cover the positive charge due to higher loading of the nucleic acid. The coating was screened by incubation of BNRplex in various concentrations of SA. SA coatings in SA solutions with concentration of 0.5−4 mg/mL increased the diameter of the complex from 190 to 220 nm and also altered the surface charge from positive (+23 mV) to negative (−5 mV) with potential to reduce toxicity *in vivo* (Fig. 1C and D). Typically, positively charged nanoparticles are known to induce toxicity *in vivo*, whereas nanoparticles with negative charge of approximately −7 mV, similar to the charge of cell sruface, have little toxicity[21,23]. Herein, SA-BNRplex with a CLG/RNA/SA mass ratio of 32:1:4 and zeta potential of −5 mV was selected for further use. The optimized SA-BNRplex formulation appears as a light yellow and

transparent liquid (Fig. 1K) and the particles in the formulation have a rod-shape with a mean diameter of approximately 150 nm (Fig. 1F). Stability test displayed that the band of anti-miR155 in the nanoparticles was still observed at 12 h after incubation with medium-containing RNase or 10% FBS at 37 °C, while the one corresponding to naked anti-miR155 completely disappeared (Fig. 1G and H). Furthermore, the size of the nanoparticles was not altered after a 12-h incubation in 10% FBS at 37 °C (Fig. 1I). The results indicated that SA-BNRplex is stable in body fluids. *In vitro* release test shows that the small molecular drug, baicalein, was released over time in a 24-h period at pH values of 7.4 and 6.8, whereas it was released faster at pH 5 since the drug is weakly basic and possesses higher solubility in acid condition (Fig. 1J).

3.2. *Efficient macrophage targeting with sustained release over time*

To investigate the targeting ability of SA-BNRplex to SA receptors on macrophages, the uptake of the various nanoparticles was examined by CLSM and flow cytometry. Cy5-RNA exhibits little red fluorescence in the cells, whereas Cy5-labeled BNRplex or SA-BNRplex displays intense fluorescence around the nucleus (Fig. 2A). Moreover, the fluorescence from the cells treated with SA-BNRplex is stronger than that treated with BNRplex. Quantification assay by flow cytometry confirms the CLSM study (Fig. 2B). Therefore, SA coating on BNRplex is able to improve their ability for macrophage-targeting.

We previously reported that rod-shaped drug particles, also named as drug nanorods, had the ability to enter cells *via* caveolar pathway, wihtout being detained by the endo-lysosomes, and facilitate intracellular delivery of biological drugs such as miRNA and active proteins[21−24]. The present SA-BNRplex has rod-like in morphology. Accordingly, it was hypothesized that the nanoparticles could be internalized through a similar pathway. The uptake study was performed in cells pretreated with M-CD, a well known inhibitor of caveolar endocytosis[24]. Pretreatment with M-CD induced 50% reduction in the uptake of the nanoparticles while the energy inhibitors, NaN_3+DG, did not affect the uptake, thereby implying the caveolae-mediated internalization with energy-indepedence (Supporting Information Fig. S2A). To confirm the caveolar endocytosis, cellular trafficking of the nanoparticles was studied after Cave-1, a specific protein involved in the formation of the caveolae, was stained with Alexa Fluor 488 (green). Yellow spots present in the merged image demonstrated the colocalization of caveolae with Cy5-labeled SA-BNRplex (Fig. S2B). Besides Cave-1, caveolar trafficking is also closely linked to the other two proteins, the actin cytoskeleton and cholera toxin subunit B (CTB)[21]. As expected, the Cy5-labeled nanoparticles colocalized well with the two proteins (Fig. S2B). In general, caveolae-mediated uptake enables the materials to enter cells *via* bypassing the endo-lysosomes[21]. As depicted in Supporting Information Fig. S3, little colocalization of these rod-shaped nanoparticles with the lysosomes was seen at 4 h after incubation. Overall, SA-BNRplex enables cellular entry without lysosomal sequestration and is promising to improve intracellular delivery of anti-miR 155.

Not being detained by the lysosomes, SA-BNRplex would be present in the cytoplasma as intact particles after uptake. However, to bind their targets, the drugs must dissociate from the nanoparticles inside the cells. The intracellular fate of internalized SA-BNRplex was then explored by incorporating an AIE dye, TPE, that emits fluorescence in the aggregate state with the fluorescence quenching when baicalein crystals in the SA-BNRplex disintegrate[29]. The fluorescence quenching is directly correlated to the disintegration of the TPE-labeled nanoparticles. As displayed in Supporting Information Fig. S4A, the nanoparticles have been uptaken by cells at 2 h after incubation, whereas the fluorescence declines after 2-h incubation, implying their disintegration. At 4 h post incubation, the fluorescence intensity decreases remarkablely, indicating considerable decomposition of the nanoparticles, and almost disappears at 7 h. CLSM examination confirms the quantification (Fig. S4B) and these results reveal that the internalized nanoparticles take approximately 7 h to release their loaded cargos.

3.3. *Efficient transfection and anti-AS effect in vitro*

The cytotoxicity of the drug-loaded formulations was first assessed against RAW 264.7 cells after 48-h incubation. CLG is a material used to stabilize BNRs in SA-BNRplex. Even at high concentration (500 μg/mL) CLG displayed little cytotoxicity (Supporting Information Fig. S5A). Incubation with various

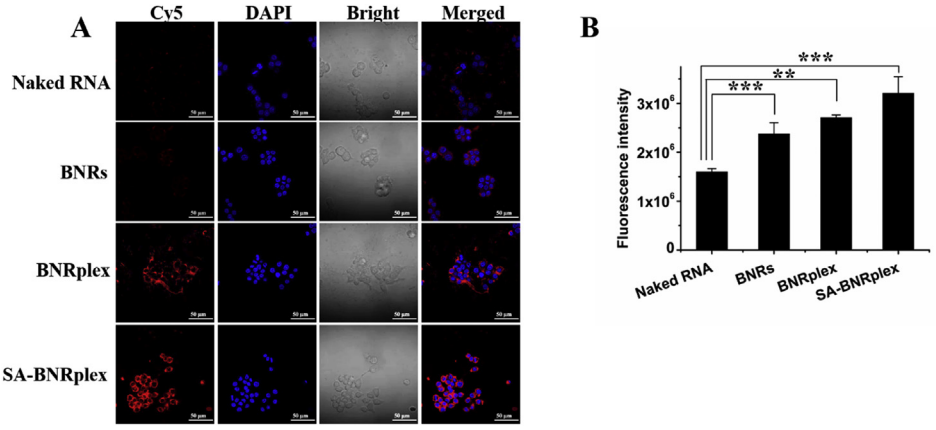

Figure 2 Macrophage targeting. Cellular uptake of Cy5-labeled nanoparticles in RAW 264.7 cells examined by (A) CLSM and (B) flow cytometry. The cells were incubated with the nanoparticles at a Cy5 concentration of 100 nmol/L at 37 °C for 4 h (mean ± SD, $n = 3$, $^{**}P < 0.01$ and $^{***}P < 0.001$). Scale bar = 50 μm.

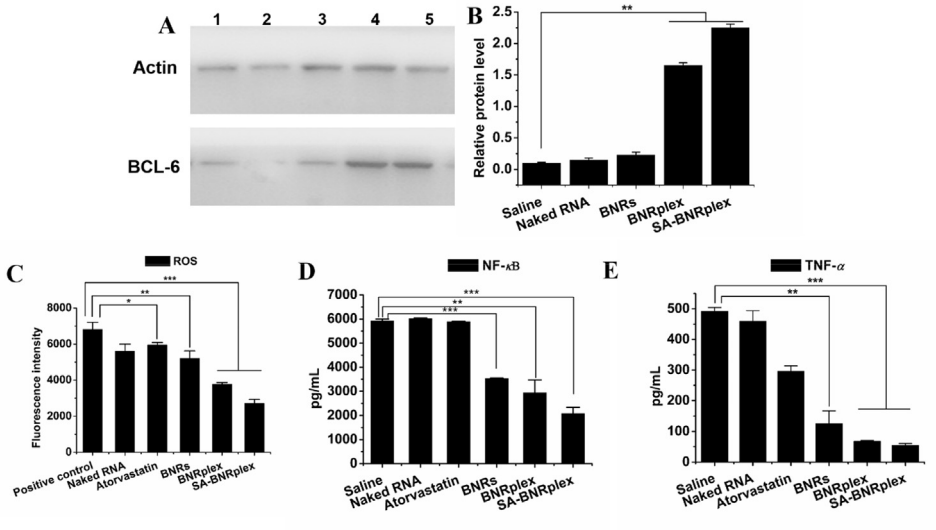

Figure 3 Transfection (A and B) and anti-inflammatory activity (C−E) *in vitro*. BCL-6 expression in RAW 264.7 cells determined by (A) WB assay and (B) quantitative analysis ($n = 3$, $^{**}P < 0.01$). (C) ROS, (D) NF-κB, and (E) TNF-α expression in RAW 264.7 cells (mean ± SD, $n = 3$, $^{*}P < 0.05$, $^{**}P < 0.01$ and $^{***}P < 0.001$). The internal control for normalizing protein expression was β-actin. Formulations: 1, saline; 2, Naked RNA; 3, BNRs; 4, BNRplex; 5, SA-BNRplex. The cells were incubated with formulations at concentrations of 60 μg/mL for baicalein, 10 μg/mL for atorvastatin, or 100 nmol/L for anti-miR 155 for 24 h at 37 °C.

formulations loaded with baicalein and anti-miR 155 at baicalein concentrations ranging from 0.25 to 500 μg/mL did not affect the cell viability as well (Fig. S5B), demonstrating their biocompatibility *in vitro*.

Having demonstrated SA-BNRplex was not entrapped within the endo-lysosomes, it was postulated their ability to efficiently deliver the loaded anti-miR 155 into the cytoplasma. First, the transfection efficacy by anti-miR155 was studied by determining the expression of targeted protein, BCL-6[30,31]. SA-BNRplex increases the intracellular level of BCL-6 by approximately 10-fold in comparison with free naked RNA (Fig. 3A and B), demonstrating effective intracellular delivery of the nucleic acid and efficient transfection. Next, the anti-inflammatory activity in RAW 264.7 cells was investigated after administration of the various formulations. The phenotypic switch from M1 to M2 was assessed by detecting two markers, CD206 and INOS, that are always highly expressed on M2 and M1, respectively[32]. Administration of drug-loaded formulations in M1 upregulates CD206 (Fig. 4A and B) and downregulates INOS, determined by CLSM observation and flow cytometry, whereas pronounced efficacy is observed in the cells treated with SA-BNRplex (Fig. 4C and D). Compared to the classical anti-AS drug in clinical use, atorvastatin, the anti-inflammatory drug nanocrystals, BNRs, allow significant enhancement in the regulation of the two markers. Notably, BNRplex and SA-BNRplex, both loading anti-miR155, are able to increase the expression of CD206 or reduce the expression of INOS over BNRs, revealing that intracellular delivery of anti-miR155 allows improved regulation of the two markers. These results indicate that codelivery of anti-inflammatory drug and anti-miRNA with SA-BNRplex enables efficient switch from M1 to M2. Due to the switch to anti-inflammatory phenotype, the secretion of inflammatory cytokines, ROS, NF-κB and TNF-α, were reduced by 1-, 3- and 10-fold, respectively, compared to the positive control after administration of SA-BNRplex (Fig. 3C−E). Overall, SA-BNRplex possesses potent anti-AS activities *in vitro*.

3.4. *Prolonged blood circulation and plaque targeting*

Due to the plaque localization at the vessel wall, blood circulation of DDS in the blood is essential for their accumulation in the plaque. Accordingly, pharmacokinetic studies of the nanoparticles were performed by intravenous injection of DiR-labeled nanoparticles (BNRs, BNRplex and SA-BNRplex) in the animal model. The plasma concentration of the nanoparticles was measured by detecting the fluorescence of DiR. The nanoparticles exhibit extremely high fluorescence for 24 h over free DiR (Fig. 5A). Even at 24 h after administration, significant fluorescence signal was still observed. Pharmacokinetic parameters were further calculated based on the plasma concentration (Fig. 5B). The $t_{1/2}$ of blood circulation from these nanoparticles is extended by approximately 45-fold, while the clearance, a pharmacokinetic measurement of the volume of plasma from which a substance is completely removed per unit time, was reduced by 4-fold. These data demonstrate that these nanoparticles are able to circulate in the blood over extended times.

Next, the accumulation of these nanoparticles in the plaque was investigated by observing the colocalization of FITC-labeled nanoparticles within the aortas. Intense pink fluorescence was observed in the merged picture in the group treated with SA-BNRplex, indicating efficient accumulation of the nanoparticles in the plaque (Fig. 5C).

3.5. *Efficient anti-AS in vivo*

The anti-AS efficacy of the different formulations was investigated in AS rat model, by analyzing artery lumen diameter, blood pressure, phenotypic switch, inflammatory factors and level of blood lipids post their injection. The drug-loaded formulations promote increase in the artery lumen diameter, but this effect was more evident in the animals treated with SA-BNRplex (Fig. 6A and B). Compared to the conventional anti-AS drug, atorvastatin,

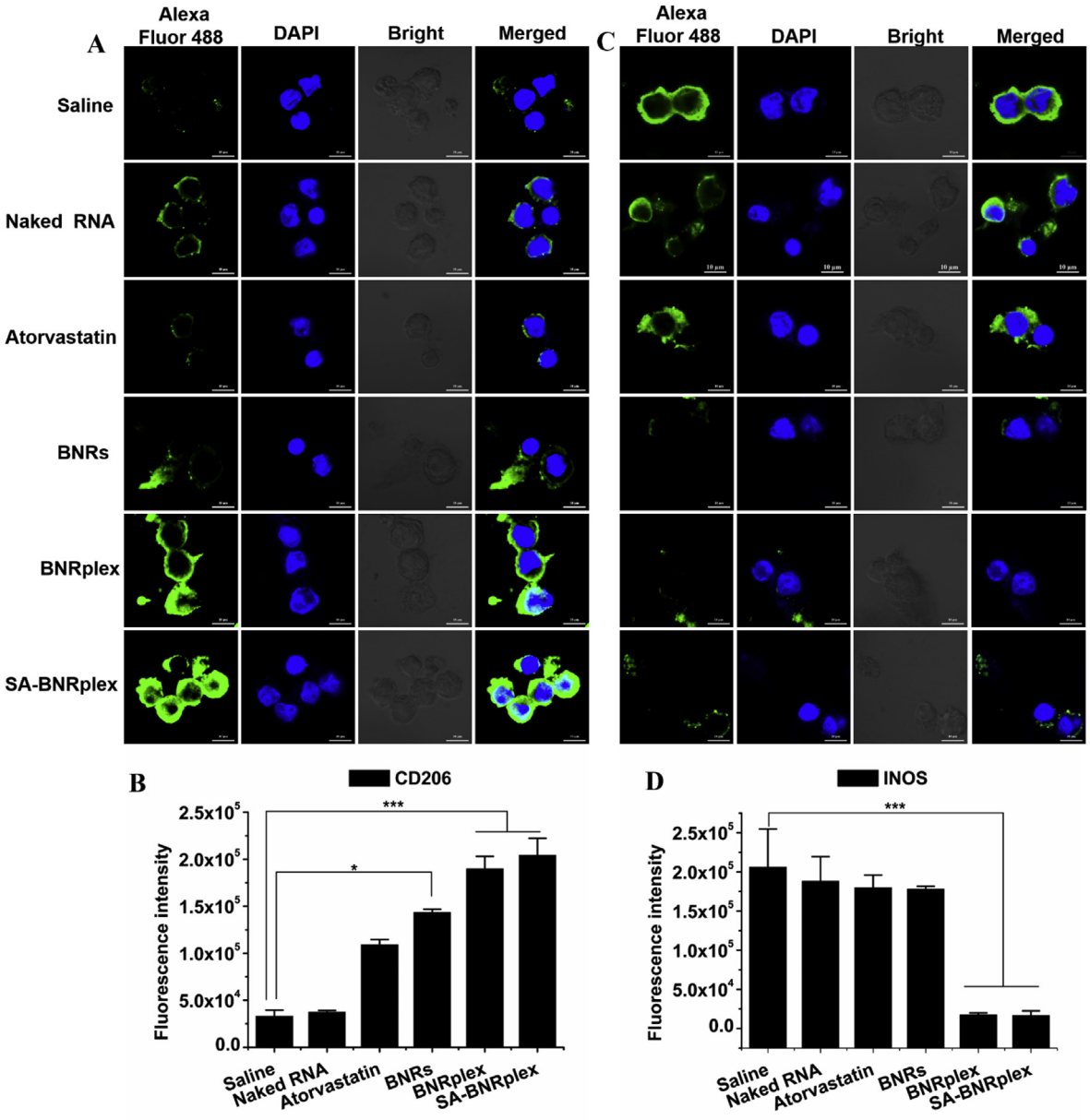

Figure 4 Phenotypic shift study *in vitro*. Immunofluorescence and quantitative analysis of CD206 (A) and (B) and INOS (C) and (D) expression on RAW 264.7 cells after treatment (mean ± SD, $n = 3$, $^{*}P < 0.05$ and $^{***}P < 0.001$). The nuclei were stained with DAPI (blue) and CD206 and INOS were stained with Alexa Fluor 488-conjugated antibody (green). The scale bar is 10 μm. The cells were incubated with the formulations at drug concentrations of 60 μg/mL (baicalein), 10 μg/mL (atorvastatin), or 100 nmol/L of anti-miR 155 for 12 h at 37 °C.

the anti-inflammatory nanoparticles, BNRs, are able to promote increased diameter of the artery lumen. Notably, codelivery of baicalein and anti-miR 155 with SA-BNRplex causes further increase in the diameter over BNRs. As a consequence of the increased artery lumen diameter, the blood pressure was significantly reduced compared with the saline group (Fig. 6C). In particular, administration of SA-BNRplex induced over 40% of decrease in the blood pressure. These outcomes derive from the efficient *in vivo* transfection of anti-miR155 (Supporting Information Fig. S6) and the resultant phenotypic switch from pro-inflammatory M1 to anti-inflammatory M2 *in vivo*. As shown in Fig. S6, SA-BNRplex elevates the expression of the targeted protein, BCL-6, by 9-folds over BNRs.

To determine the phenotypic conversion, the tissues in the lesional area were collected at the end of treatment and were sectioned for staining the markers CD206 and INOS, that are usually overexpressed on M2 and M1, respectively. Codelivery formulations, BNRplex and SA-BNRplex, enable significant increase in the expression of CD206 (Fig. 7A and B) and reduction in the expression of INOS (Fig. 7C and D). Again, BNRs could regulate the two markers with higher efficacy compared to atorvastatin, being in accordance with the *in vitro* results. These findings indicate that codelivery of baicalein and anti-miR 155 with SA-BNRplex effectively promots the M1−M2 switch *in vivo*.

Inflammation is known to influence the onset and development of AS[7,33]. As expected, the inflammatory factors in the aortas,

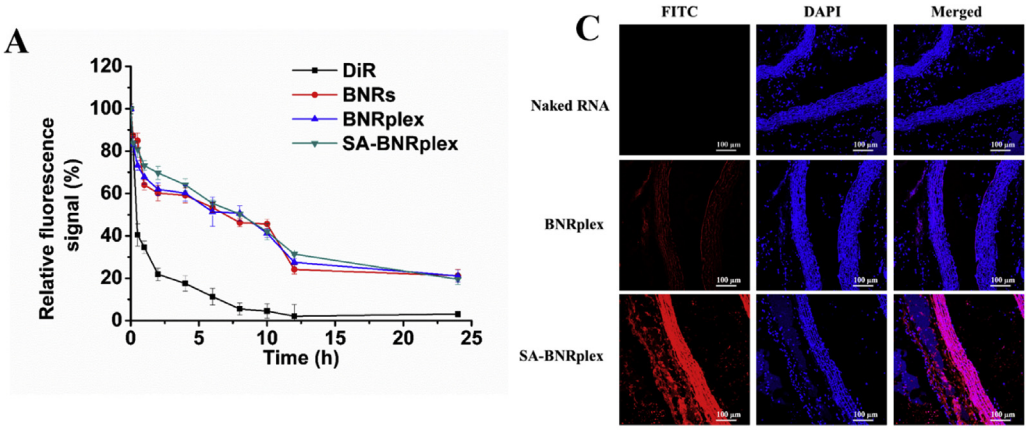

B

Parameters	Free DiR	BNRs	BNRplex	SA-BNRplex
AUC (μg/L·h)	3.14±0.12	13.28±1.23	13.20±0.45	13.34±0.13
$t_{1/2}$ (h)	0.31±0.08	13.61±0.13	13.29±0.15	15.04±0.25
T_{max} (h)	0.17±0.00	0.17±0.00	0.17±0.00	0.17±0.00
CL (L/h/g)	1.61±0.02	0.38±0.03	0.38±0.01	0.38±0.03

Figure 5 Blood circulation and plaque targeting. (A) Plasma concentration−time curves and (B) pharmacokinetic parameters. DiR-labeled nanorods were injected *via* the tail vein at the DiR dose of 0.5 mg/kg, according to the body weight (mean ± SD, $n = 5$). (C) Colocalization of FITC-labeled nanorods and aortas. The artery vessels were collected at 2 h post injection of FITC-labeled nanorods at a FITC dose of 0.25 mg/kg. The nuclei were stained by DAPI (blue). The scale bar is 100 μm. C_{max}, maximum plasma concentration; AUC, area under the concentration curve; T_{max}, time to reach Cmax; $t_{1/2}$, biological half-life; CL, clearance.

including NF-κB, TNF-α and ROS, were downregulated remarkably after dosing BNRs, BNRplex or SA-BNRplex (Fig. 6D−F). Especially, dosing SA-BNRplex reduced these factors by approximately 4-folds for NF-κB, 9-folds for TNF-α, and 3.5-folds for ROS, demonstrating considerable inhibition of the inflammatory response.

Lipid accumulation is a well-known cause and a strong driver of AS and always results in formation of foam cells in the plaque[33]. Increased plasma triglyceride (TG), total cholesterol (TC) and low density lipoprotein (LDL) levels are closely correlated to the development of AS[34]. Herein, serum lipid profile was examined by measuring the three index at the end of the treatment (Fig. 6G and I). Atorvastatin is a anti-AS drug that lowers the blood lipids. SA-BNRplex enables lower levels of LDL and TC and similar level of TG compared to atorvastatin. Overall, codelivery of baicalein and anti-miR 155 with SA-BNRplex lowers the blood lipids significantly.

4. Discussion

Baicalein nanorods (BNRs) allow for potent inflammation inhibition *in vitro* and *in vivo*, as shown by suppression of ROS, NF-κB and TNF-α. Baicalein is known to inhibit inflammation responses by blocking mutilple pathways such as estrogen receptor and NF-κB-dependent pathways[35] and impairment of production of reactive oxygen intermediate through antagonizing ligand-initiated Ca^{2+} influx[36]. However, no reports have shown its ability to faciliate the phenotypic switch of macrophages. Herein, dosing BNRs upregulates CD206 and downregulates INOS on RAW 264.7 cells compared with administration of saline, implying polarization of M1 toward M2 (Figs. 4 and 6). Atorvastatin is a drug frequently used in the clinic to treat AS. Recently, it was demonstrated that the drug confers anti-inflammation activity[37,38]. By contrast, BNRs exhibit improved ability of polarization compared to atorvastatin. Macrophages continuously adapt their polarization in response to the surrounding conditions, but this ability is compromised when conventional dosage forms with fast drug release profiles are used[7]. Intracellular fate assay reveals that the drug nanorods are capable of continuously release the drug in a 7-h period. Accordingly, the sustained release from BNRs over time contributes to the enhanced polarization. Overall, nanocrystal approach is a promising formulation method to improve the potency of an anti-inflammatory drug due to the sustained release over time after internalization.

Intracellular delivery of anti-miR 155 with baicalein nanorods (BNRs) effectively promotes polarization of M1 toward M2 *in vitro* and *in vivo*. MiR-155 is a common target to mediate inflammation and it plays a critical role in atherogenic programming of macrophages to sustain and enhance vascular inflammation by derepressing BCL-6-mediated inhibition of recombinant mouse monocyte chemotactic protein-1 (CCL2) transcription[11,12]. Therefore, intracellular delivery of miR155 antagonist, anti-miR155, holds the potential to inhibit inflammation in macrophages and treat AS. Nonetheless, cytosolic delivery of biologics with conventional drug carriers is challenging due to degradation in the endo-lysosomes[39]. Less than 0.25-fold increase in transfection efficacy was reported when employing acid-labile polyethylenimine (acid-labile PEI) as a carrier to deliver anti-miR155 to RAW 264.7 cells *via* endo-lysosomal route[40]. By contrast, BNRplex allows increase of the trasfection efficacy *in vitro* and *in vivo* by > 10- and >5-fold, respectively, compared with naked RNA. By targeting the SA receptors on RAW 264.7 cells, SA-

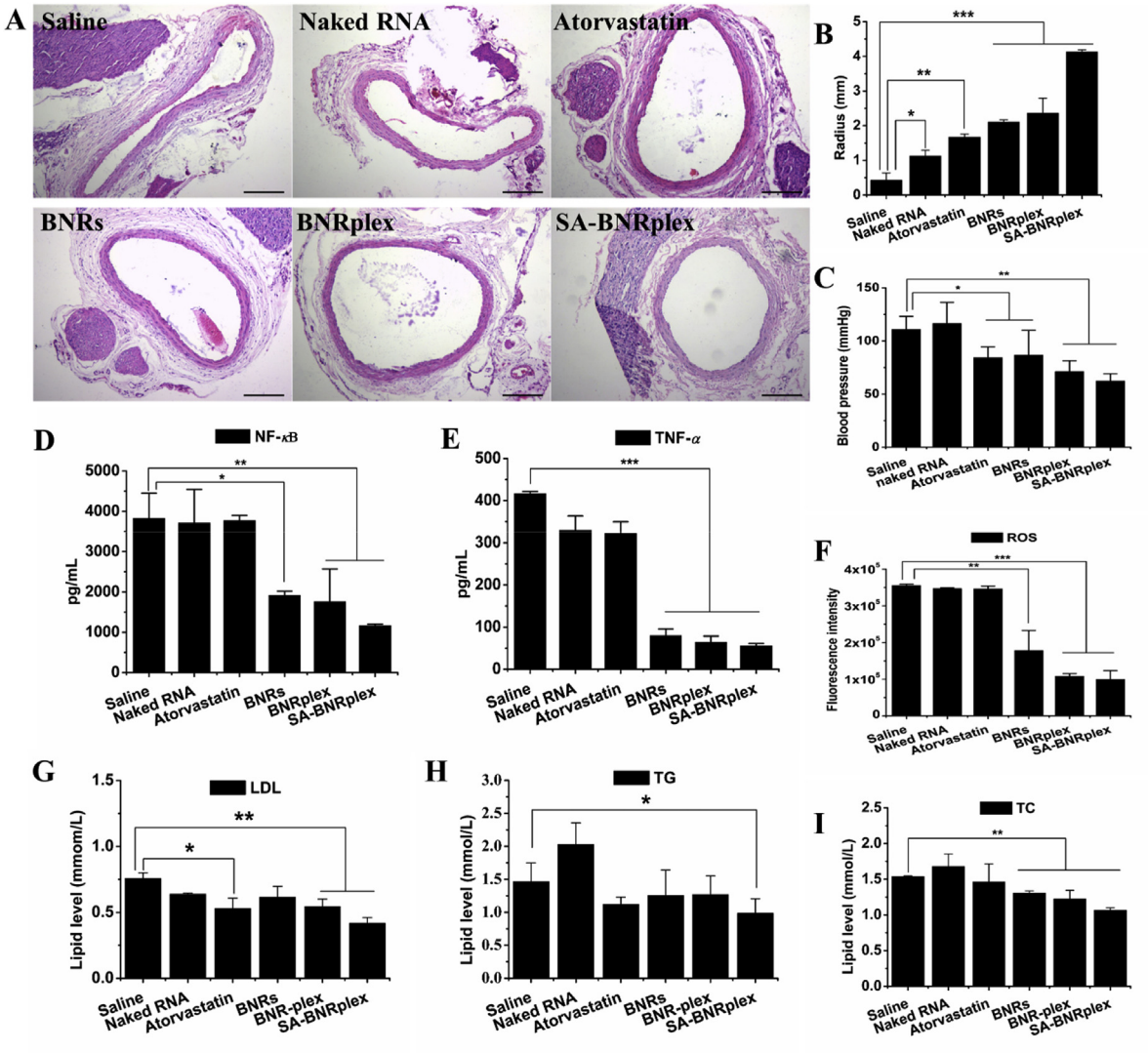

Figure 6 Anti-AS activities *in vivo*. Artery lumen diameter determination. (A) H&E staining and (B) quantitative assay (mean ± SD, $n = 5$, $^{*}P < 0.05$, $^{**}P < 0.01$ and $^{***}P < 0.001$). The scale bar is 100 μm. Determinations of (C) systemic blood pressure, (D)−(F) inflammatory factors in aortas, and (G)−(I) serum lipid profile at the end of the treatment (mean ± SD, $n = 5$, $^{*}P < 0.05$, $^{**}P < 0.01$ and $^{***}P < 0.001$). The formulations (0.2 mL), saline, naked RNA, atorvastatin, BNRs, BNRplex, SA-BNRplex, were injected into the animals *via* the tail vein every 3 days at a baicalein dose of 5 mg/kg, anti-miR 155 dose of 0.2 mg/kg, or atorvastatin dose of 1 mg/kg, according to the body weight.

BNRolex increased the transfection efficacy by approximately 17- and 8-fold over naked RNA, respectively. The efficient transfection was possible thanks to the internalization of SA-BNRplex *via* bypassing the endo-lysosomes, as demonstrated in Fig. S2. Surprisingly, intracellular delivery of anti-miR155 with SA-BNRplex markedly upregulated the marker of anti-inflammatory macrophages (M2) and downregulated the marker of pro-inflammatory phenotype (M1), unvealing promotion of M2 polarization of macrophages. It is well known that M1 polarization of macrophages is involved in the intiation and development of various inflammatory diseases, such as cardiovascualr diseases (AS, pulmonary arterial hypertension, myocarditis, and myocardial infarction), rheumatoid arthritis, and inflammatory bowel disease[7]. It is then likely that SA-BNRplex technology could be generally applied for the treatment of inflammatory diseases.

Targeting the dissamilated plaque at the vascular wall is always challenging for conventional DDS such as solid lipid nanoparticles and polymer micelles due to their short life in circulation[7,41,42]. SA-BNRplex with a rod-like morphology is capable of accumulating in the plaque after intraveneous injection. The higher surface of rod-shaped nanoparticles compared to spherical particles enables enhanced capability to marginate and adhere to the vascular wall[43]. Furthermore, prolonged blood circulation and active targeting to macrophages improve accumulation of the nanoparticles in the plaques (Figs. 2A and 5A**).** In fact, rod-shaped nanoparticles have shown enhanced tissue-penetration property contributing for the plaque accumulation[24].

Codelivery of baicalein and anti-miR 155 by DDD strategy is efficient to treat AS in animal model. Macrophage-targeting to promote M2 polarization is a promising strategy to delay the development of AS, owing to inhibition of inflammation response and prevention of plaque rupture[44]. Inhibiting the secretion of pro-inflammatory factors, such as ROS, TNF-α, and IL-1β, from macrophages has been demonstrated to regress

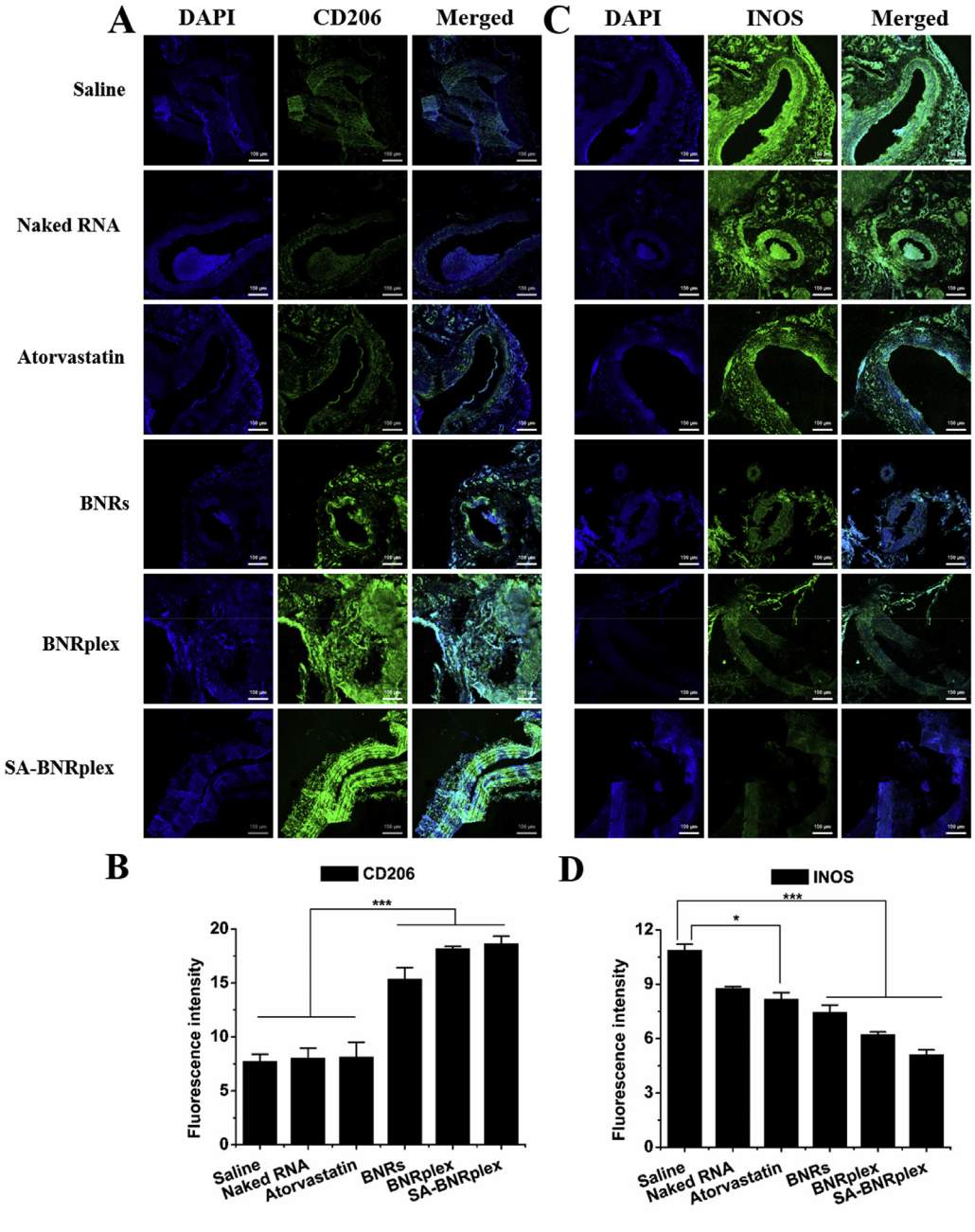

Figure 7 Study of phenotypic shift *in vivo*. Immunofluorescence and quantitative analysis of CD206 (A) and (B) and INOS (C) and (D) expression on sectioned plaque collected after treatment (mean ± SD, $n = 3$, $^{*}P < 0.05$ and $^{***}P < 0.001$). The nuclei were stained with DAPI (blue) and CD206 and INOS were stained with Alexa Fluor 488-conjugated antibody (green). The scale bar is 100 μm. The formulations were injected into the animals *via* the tail vein every 3 days at a baicalein dose of 5 mg/kg, anti-miR 155 dose of 0.2 mg/kg, or atorvastatin dose of 1 mg/kg, according to the body weight.

AS[45,46]. SA-BNRplex polarized macrophages toward M2 phenotype and effectively inhibited secretion of pro-inflammatory factors, NF-κB, TNF-α and ROS, *in vitro* and *in vivo*. The robust anti-AS activities is also ascribed to the extremely high drug-loading capacity of SA-BNRplex. Commonly used nanoparticles have in general a payload capacity of less than 10%[47]. Here, the present nanoparticles possess drug-loading over 80% in total, which corresponds to a 8-fold increase. The polarization of macrophages in particular requires the design of durable therapeutic interventions as they can easly repolarized by the surrounding microenvironment[7,48]. For frequently used nanoparticles, like liposomes and micelles[49,50], the entrapment in the lysosomes during the internalization process decomposes the nanoparticles rapidly and enables short-time drug exposure[39]. The nanoparticles developed and investigated in this study allow sustained release over up to 7 h after cytosolic delivery *via* bypassing the endo-lysomses and provide a more robust effect to regulate the polarization of

macrophages. So far, few reports have described nanoparticles with the ability for controlled drug release post-internalization[51]. Additionally, administration of SA-BNRplex promotes improved reduction in the blood lipids over atorvastatin, a classical anti-AS drug. Lipid accumulation in the plaque directs macrophages toward M1 pro-inflammatory phenotype and facilitates formation of foam cells[52]. Accordingly, the reduced blood lipids may be ascribed to the promotion of the M2 polarization induced by the nanoparticles. Taken together, the potency of SA-BNRplex to treat AS results from the ability of plaque targeting, promoted M2 polarization, high drug-loading capacity, efficient intracellular delivery of anti-miR155 and sustained release after internalization. This delivery platform is promising and can be easily translated to the clinic due to its simple preparation process and scalability.

5. Conclusions

By using a DDD strategy, anti-inflammatory baicalein nanocrystals were utilized as carriers for intracellular delivery of nucleic acids, a combined platform to codeliver an anti-inflammatory drug and anti-miR 155 to treat inflammatory disease *via* targeting to macrophages. The platform promotes M2 polarization and inhibit inflammatory activities *in vitro* and *in vivo,* owing to the extremely high drug-loading capacity, sustained drug release and the resulting durable response after internalization. In particular, due to prolonged blood circulation and improved accumulation at the inflammation site on the vascular wall, the codelivery platform allows for efficent treatment of AS by increasing the diameter of artery lumen, lowering blood pressure, facilitating phenotypic switch, suppressing release of inflammatory factors and reducing blood lipids. Overall, the macrophage-targeted platform is potent to polarize macrophages and alleviate inflammation and is able to be employed as a common approach to combat vascular inflammation.

Acknowledgments

This study was supported by the National Natural Science Foundation of China (Nos. 81872823 and 81773826), the Double First-Class (CPU2018PZQ13, China) of the China Pharmeutical University, the Ministry of Science and Technology of China (2018ZX09711001), the Shanghai Science and Technology Committee (19430741500, China), and the Key Laboratory of Modern Chinese Medicine Preparation of Ministry of Education of Jiangxi University of traditional Chinese Medicine (TCM-201905, China).

Author contributions

Wei He conceived and designed the research work. Chao Teng, Chenshi Lin, Feifei Huang, Xuyang Xing, Shenyu Chen, Ling Ye, Helena S. Azevedoo, Chenjie Xu, Zhengfeng Wu, Zhongjian Chen perdromed the experiments. Wei He and Chao Teng co-wrote the paper. All of the authors discussed the results and commented on the manuscript. All of the authors have read and approved the final manuscript.

Conflicts of interest

The authors have no conflicts of interest to declare.

Appendix A. Supporting information

Supporting data to this article can be found online at https://doi.org/10.1016/j.apsb.2020.06.005.

References

1. Kasikara C, Doran AC, Cai B, Tabas I. The role of non-resolving inflammation in atherosclerosis. *J Clin Invest* 2018;**128**:2713–23.
2. Tian L, Lu L, Feng J, Melancon MP. Radiopaque nano and polymeric materials for atherosclerosis imaging, embolization and other catheterization procedures. *Acta Pharm Sin B* 2018;**8**:360–70.
3. Weber C, Noels H. Atherosclerosis: current pathogenesis and therapeutic options. *Nat Med* 2011;**17**:1410.
4. Basatemur GL, Jørgensen HF, Clarke MC, Bennett MR, Mallat Z. Vascular smooth muscle cells in atherosclerosis. *Nat Rev Cardiol* 2019;**16**:727–44.
5. Jin K, Luo Z, Zhang B, Pang Z. Biomimetic nanoparticles for inflammation targeting. *Acta Pharm Sin B* 2018;**8**:23–33.
6. Moore KJ, Tabas I. Macrophages in the pathogenesis of atherosclerosis. *Cell* 2011;**145**:341–55.
7. He W, Kapate N, Shields IV CW, Mitragotri S. Drug delivery to macrophages: a review of targeting drugs and drug carriers to macrophages for inflammatory diseases. *Adv Drug Deliv Rev* 2019. Available from: https://doi.org/10.1016/j.addr.2019.12.001.
8. Mosser DM. The many faces of macrophage activation. *J Leukoc Biol* 2003;**73**:209–12.
9. Abid S, Marcos E, Parpaleix A, Amsellem V, Breau M, Houssaini A, et al. CCR2/CCR5-mediated macrophage-smooth muscle cell crosstalk in pulmonary hypertension. *Eur Respir J* 2019;**54**:1802308.
10. Cai X, Yin Y, Li N, Zhu D, Zhang J, Zhang CY, et al. Re-polarization of tumor-associated macrophages to pro-inflammatory M1 macrophages by microRNA-155. *J Mol Cell Biol* 2012;**4**:341–3.
11. O'Connell RM, Taganov KD, Boldin MP, Cheng G, Baltimore D. MicroRNA-155 is induced during the macrophage inflammatory response. *Proc Natl Acad Sci U S A* 2007;**104**:1604–9.
12. Nazari-Jahantigh M, Wei Y, Noels H, Akhtar S, Zhou Z, Koenen RR, et al. MicroRNA-155 promotes atherosclerosis by repressing Bcl-6 in macrophages. *J Clin Invest* 2012;**122**:4190–202.
13. Leitinger N, Schulman IG. Phenotypic polarization of macrophages in atherosclerosis. *Arterioscl Throm Vas* 2013;**33**:1120–6.
14. Patwardhan RS, Sharma D, Thoh M, Checker R, Sandur SK. Baicalein exhibits anti-inflammatory effects *via* inhibition of NF-κB transactivation. *Biochem Pharmacol* 2016;**108**:75–89.
15. He X, Wei Z, Zhou E, Chen L, Kou J, Wang J, et al. Baicalein attenuates inflammatory responses by suppressing TLR4 mediated NF-κB and MAPK signaling pathways in LPS-induced mastitis in mice. *Int Immunopharm* 2015;**28**:470–6.
16. Zhang X, Tian H, Wu C, Ye Q, Jiang X, Chen L, et al. Effect of baicalin on inflammatory mediator levels and microcirculation disturbance in rats with severe acute pancreatitis. *Pancreas* 2009;**38**:732–8.
17. He W, Xing X, Wang X, Wu D, Wu W, Guo J, et al. Nanocarrier-mediated cytosolic delivery of biopharmaceuticals. *Adv Funct Mater* 2020. Available from: https://doi.org/10.1002/adfm.201910566.
18. Wu W, Li T. Unraveling the *in vivo* fate and cellular pharmacokinetics of drug nanocarriers. *Adv Drug Deliv Rev* 2019;**143**:1–2.
19. Lv Y, Xu C, Zhao X, Lin C, Yang X, Xin X, et al. Nanoplatform assembled from a CD44-targeted prodrug and smart liposomes for dual targeting of tumor microenvironment and cancer cells. *ACS Nano* 2018;**12**:1519–36.
20. Gilleron J, Querbes W, Zeigerer A, Borodovsky A, Marsico G, Schubert U, et al. Image-based analysis of lipid nanoparticle-mediated siRNA delivery, intracellular trafficking and endosomal escape. *Nat Biotechnol* 2013;**31**:638–46.

21. Xin X, Du X, Xiao Q, Azevedo HS, He W, Yin L. Drug nanorod-mediated intracellular delivery of microRNA-101 for self-sensitization *via* autophagy inhibition. *Nano-Micro Lett* 2019;**11**:82.
22. Xin X, Pei X, Yang X, Lv Y, Zhang L, He W, et al. Rod-shaped active drug particles enable efficient and safe gene delivery. *Adv Sci* 2017;**4**:1700324.
23. Xin X, Teng C, Du X, Lv Y, Xiao Q, Wu Y, et al. Drug-delivering-drug platform-mediated potent protein therapeutics *via* a non-endo-lysosomal route. *Theranostics* 2018;**8**:3474−89.
24. He W, Xin X, Li Y, Han X, Qin C, Yin L. Rod-shaped drug particles for cancer therapy: the importance of particle size and participation of caveolae pathway. *Part Part Syst Char* 2017;**34**:1600371.
25. Castaneda-Roldan EI, Avelino-Flores F, Dall'Agnol M, Freer E, Cedillo L, Dornand J, et al. Adherence of *Brucella* to human epithelial cells and macrophages is mediated by sialic acid residues. *Cell Microbiol* 2004;**6**:435−45.
26. Crocker PR, Mucklow S, Bouckson V, McWilliam A, Willis AC, Gordon S, et al. Sialoadhesin, a macrophage sialic acid binding receptor for haemopoietic cells with 17 immunoglobulin-like domains. *EMBO J* 1994;**13**:4490−503.
27. Pang J, Xu Q, Xu X, Yin H, Xu R, Guo S, et al. Hexarelin suppresses high lipid diet and vitamin D3-induced atherosclerosis in the rat. *Peptides* 2010;**31**:630−8.
28. Gou SH, Liu BJ, Han XF, Wang L, Zhong C, Liang S, et al. Anti-atherosclerotic effect of *Fermentum rubrum* and *Gynostemma pentaphyllum* mixture in high-fat emulsion-and vitamin D3-induced atherosclerotic rats. *J Chin Med Assoc* 2018;**81**:398−408.
29. Wang Y, Zhang Y, Wang J, Liang XJ. Aggregation-induced emission (AIE) fluorophores as imaging tools to trace the biological fate of nano-based drug delivery systems. *Adv Drug Deliv Rev* 2019;**143**:161−76.
30. Sandhu SK, Volinia S, Costinean S, Galasso M, Neinast R, Santhanam R, et al. miR-155 targets histone deacetylase 4 (HDAC4) and impairs transcriptional activity of B-cell lymphoma 6 (BCL6) in the Eμ-miR-155 transgenic mouse model. *Prog Nat Sci* 2012;**109**:20047−52.
31. Bruen R, Fitzsimons S, Belton O. miR-155 in the resolution of atherosclerosis. *Front Pharmacol* 2019;**10**:463.
32. Martinez FO, Gordon S. The M1 and M2 paradigm of macrophage activation: time for reassessment. *F1000 Prime Reports* 2014;**6**:13.
33. Tabas I, Bornfeldt KE. Macrophage phenotype and function in different stages of atherosclerosis. *Circ Res* 2016;**118**:653−67.
34. Nagareddy PR, Murphy AJ, Stirzaker RA, Hu Y, Yu S, Miller RG, et al. Hyperglycemia promotes myelopoiesis and impairs the resolution of atherosclerosis. *Cell Metabol* 2013;**17**:695−708.
35. Fan GW, Zhang Y, Jiang X, Zhu Y, Wang B, Su L, et al. Anti-inflammatory activity of baicalein in LPS-stimulated raw 264.7 macrophages *via* estrogen receptor and NF-κB-dependent pathways. *Inflammation* 2013;**36**:1584−91.
36. Shen YC, Chiou WF, Chou YC, Chen CF. Mechanisms in mediating the anti-inflammatory effects of baicalin and baicalein in human leukocytes. *Eur J Pharmacol* 2003;**465**:171−81.
37. Han F, Xiao QQ, Peng S, Che XY, Jiang LS, Shao Q, et al. Atorvastatin ameliorates LPS-induced inflammatory response by autophagy *via* AKT/mTOR signaling pathway. *J Cell Biochem* 2018;**119**:1604−15.
38. Xu X, Gao W, Cheng S, Yin D, Li F, Wu Y, et al. Anti-inflammatory and immunomodulatory mechanisms of atorvastatin in a murine model of traumatic brain injury. *J Neuroinflammation* 2017;**14**:167.
39. Donahue ND, Acar H, Wilhelm S. Concepts of nanoparticle cellular uptake, intracellular trafficking, and kinetics in nanomedicine. *Adv Drug Deliv Rev* 2019;**143**:68−96.
40. Lu J, Zhao Y, Zhou X, He JH, Yang Y, Jiang C, et al. Biofunctional polymer−lipid hybrid high-density lipoprotein-mimicking nanoparticles loading anti-miR 155 for combined antiatherogenic effects on macrophages. *Biomacromolecules* 2017;**18**:2286−95.
41. Tang J, Lobatto ME, Hassing L, van der Staay S, Van Rijs SM, Calcagno C, et al. Inhibiting macrophage proliferation suppresses atherosclerotic plaque inflammation. *Sci Adv* 2015;**1**:e1400223.
42. Li C, Wang J, Wang Y, Gao H, Wei G, Huang Y, et al. Recent progress in drug delivery. *Acta Pharm Sin B* 2019;**9**:1145−62.
43. Cooley M, Sarode A, Hoore M, Fedosov DA, Mitragotri S, Gupta AS. Influence of particle size and shape on their margination and wall-adhesion: implications in drug delivery vehicle design across nano-to-micro scale. *Nanoscale* 2018;**10**:15350−64.
44. Nakashiro S, Matoba T, Umezu R, Koga J-i, Tokutome M, Katsuki S, et al. Pioglitazone-incorporated nanoparticles prevent plaque destabilization and rupture by regulating monocyte/macrophage differentiation in *ApoE*$^{-/-}$ Mice. *Arterioscl Throm Vas* 2016;**36**:491−500.
45. Wang Y, Li L, Zhao W, Dou Y, An H, Tao H, et al. Targeted therapy of atherosclerosis by a broad-spectrum reactive oxygen species scavenging nanoparticle with intrinsic anti-inflammatory activity. *ACS Nano* 2018;**12**:8943−60.
46. Beldman TJ, Senders ML, Alaarg A, Pérez-Medina C, Tang J, Zhao Y, et al. Hyaluronan nanoparticles selectively target plaque-associated macrophages and improve plaque stability in atherosclerosis. *ACS Nano* 2017;**11**:5785−99.
47. Shen Y, Jin E, Zhang B, Murphy CJ, Sui M, Zhao J, et al. Prodrugs forming high drug loading multifunctional nanocapsules for intracellular cancer drug delivery. *J Am Chem Soc* 2010;**132**:4259−65.
48. Shields IV CW, Wang LLW, Evans MA, Mitragotri S. Materials for immunotherapy. *Adv Mater* 2019:1901633.
49. Qi J, Hu X, Dong X, Lu Y, Lu H, Zhao W, et al. Towards more accurate bioimaging of drug nanocarriers: turning aggregation-caused quenching into a useful tool. *Adv Drug Deliv Rev* 2019;**143**:206−25.
50. Man F, Gawne PJ, de Rosales RT. Nuclear imaging of liposomal drug delivery systems: a critical review of radiolabelling methods and applications in nanomedicine. *Adv Drug Deliv Rev* 2019;**143**:134−60.
51. Lu Y, Lv Y, Li T. Hybrid drug nanocrystals. *Adv Drug Deliv Rev* 2019;**143**:115−33.
52. Chinetti-Gbaguidi G, Colin S, Staels B. Macrophage subsets in atherosclerosis. *Nat Rev Cardiol* 2015;**12**:10−7.